ADVANCED FUNCTIONAL MATERIALS
www.afm-journal.de

A Multifunctional Cationic Pentathiophene: Synthesis, Organelle-Selective Imaging, and Anticancer Activity

Gaomai Yang, Libing Liu, Qiong Yang, Fengting Lv, and Shu Wang**

At present, there is an urgent necessity for the discovery of new chemotherapeutic agents with novel molecular skeleton structures that exhibit wide spectrum antitumor activity. In this work, a cationic pentathiophene (5T) is synthesized and discovered to have both anticancer activity and molecular imaging property. 5T can selectively accumulate in mitochondria to exhibit organellar imaging and efficiently induce cell apoptosis associating with JNK pathway activation. Additionally, complexes are prepared through electrostatic interactions between 5T and sodium chlorambucil (a widely used anticancer drug) with varying molar ratios. The complexes form nanoparticles in water with the size of about 50 nm. The 5T-chlorambucil nanoparticles enhance anticancer activity by 2–9 fold due to the synergistical anticancer activity of 5T and chlorambucil. 5T is therefore a promising multifunctional anticancer agent that incorporates optical monitoring capability and anticancer activity that targets mitochondria.

1. Introduction

The control and therapy of cancer represents an increasingly serious global public health problem now.[1–3] The clinical approaches of cancer therapy include surgery, radiation, chemotherapy or a combination of any of these treatments. Although different kinds of anticancer methods or strategies have been developed, chemotherapy continues to be an indispensable approach for inoperable or metastatic cancers. In the treatment of cancer, the resistance to chemotherapy has accounts for the vast majority of the deaths occur every year in the world. Due to drug resistance, it has been becoming a major disadvantage for the use of typical chemotherapeutic drugs (e.g., cisplatin, thiotepa, chlorambucil, doxorubicin and paclitaxel). Recently, great attention has been paid to the multifunctional anticancer agents for simultaneous cancer imaging, diagnosis and therapy, which provides a new strategy in cancer treatment.[4,5] Thus, there is an urgent necessity for the discovery of new chemotherapeutic strategies and agents that exhibit wide spectrum antitumor activity.

G. Yang, Dr. L. Liu, Dr. Q. Yang, Dr. F. Lv, Prof. S. Wang
Beijing National Laboratory for Molecular Science
Key Laboratory of Organic Solids
Institute of Chemistry
Chinese Academy of Sciences, Beijing, 100190, P. R. China
E-mail: wangshu@iccas.ac.cn; liulibing@iccas.ac.cn

DOI: 10.1002/adfm.201101764

Very recently, a cationic polythiophene, PMNT, was first explored by us as a multifunctional agent for simultaneously cancer therapeutic and apoptosis imaging.[6] However, non-specific imaging, less efficient cytotoxicity (IC_{50} = 188 μM) and structural uncertainties in this polymer (i.e. molecular weight distribution and structural defects) limit its potential application as effective antitumor agent. With the aim to discover the anticancer drug with novel molecular skeleton structure, it occurred to us that cationic oligomers with precise structures may fulfill these criteria. In this respect, it is reported that sulfur-containing thiophene heterocyclic compounds are distributed widely among the species of the natural products and known drugs. The natural thiophene compounds are thought to play an important role in the chemical defense of plants against herbivorous insects and other pests.[7,8] The α-terthiophene derivatives are reported to show effective antitumor activity.[9,10]

In this work, a series of amphiphilic cationic oligothiophene were synthesized (**1T**, **3T** and **5T**), among which pentameric thiophene oligomer (**5T**) shows significant anticancer activity towards different kinds of human cancer cell lines. **5T** can selectively accumulate in mitochondria and efficiently induce cell apoptosis associating with JNK pathway activation. It is therefore a promising multifunctional mitochondria-directed anticancer agent that incorporates fluorescence imaging and efficient anticancer activity. Besides, cationic **5T** and negatively charged sodium chlorambucil (a widely used anticancer drug)[11] can form nanoparticles through electrostatic interactions, which greatly enhances the anticancer activity relative to **5T** and chlorambucil themselves. Thus **5T** is a promising multifunctional anticancer agent for simultaneous cancer imaging and therapy, and also provides a new strategy in cancer treatment by drug combination to improve antitumor activity.

2. Results and Discussion

Scheme 1 depicts the synthetic routes of cationic oligothiophenes **1T**, **3T** and **5T**. Reaction of compound **1** with 1, 6-dibromohexane in the presence of sodium hydride affords 3-(2-(6-bromohexyloxy)ethyl)thiophene **2** in 31% yield. Bromination of **2** with one equivalent and two equivalents of *N*-bromosuccinimide (NBS) gives **3** and **5** in 83% and 90% yields,

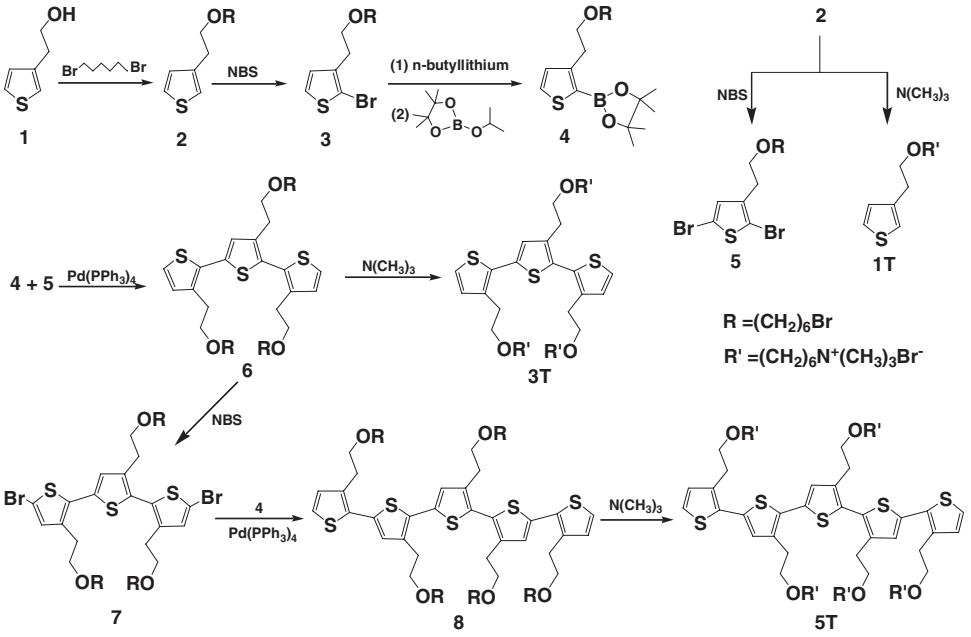

Scheme 1. The synthetic routes of cationic oligothiophenes **1T**, **3T** and **5T**.

respectively. Treatment of **3** with *n*-butyllithium at –78 °C, followed by reaction with 2-isopropoxy- 4,4,5,5,-tetramethyl-1,3,2-dioxaborolane affords 2-thienyl boronate ester **4** in 51% yield. Reaction of compound **4** and **5** via Suzuki cross-coupling in the presence of aqueous K_2CO_3 and $Pd(PPh_3)_4$ gives terthiophene **6** in 68% yield. Bromination of **6** with two equivalents of NBS in DMF affords compound **7** in 93% yield. Reaction of compound **4** and **7** via Suzuki cross-coupling gives pentathiophene **8** in 68% yield. The title compounds, cationic **1T**, **3T** and **5T** are obtained by reaction of **2**, **6** and **8** with trimethylamine in THF in 89%, 93% and 90% yields, respectively. The optical properties of **3T** and **5T** were investigated in aqueous solution, whereas **1T** does not show optical characterization. The **3T** exhibits maximum absorption at 318 nm with an extinction coefficient of 1.18×10^4 $M^{-1} \cdot cm^{-1}$. As the number of thiophene unit increases, the maximum absorption of **5T** red shifts to 361 nm with an extinction coefficient of 4.4×10^4 M^{-1} cm^{-1}. Upon excitation at the maximum absorption, the emission spectra show maximum emission at 423 nm for **3T** and 495 nm for **5T**. The fluorescence quantum yield of **5T** (Φ = 6%) is ~5-fold higher than that of **3T** (Φ = 1.2%). Thus the red shift of emission and higher quantum yield make **5T** as a probe with good fluorescence imaging ability.

The MTT method is one of the most preferred cytotoxicity tests for new anticancer agents. In this method the yellow MTT dye is reduced to insoluble formazan by mitochondrial dehydrogenases, which is related to cell viability.[12] The cytotoxicities of **1T**, **3T**, and **5T** toward five different kinds of human cancer cell lines and one normal cell line were determined by MTT after incubating cells and oligothiophenes for 48 h (**Figure 1**a and Figure S1 in the Supporting Information). The cytotoxicity of **3T** is a little higher than that of **1T**, while for **5T** with more thiophene units, it exhibits best anticancer activity (five times more cytotoxic than **1T** and **3T)**. Thus, the number of thiophene unit is responsible for the anticancer activity. The IC_{50} values of **5T** to six cell lines were calculated as shown in Figure 1b. All cell lines are sensitive to **5T** with IC_{50} in the range of 6.96 ~ 18.07 μM. It is noticeable that **5T** shows similar levels of cytotoxic activity against cancerous and normal cell line (HPF), which shows that further optimization

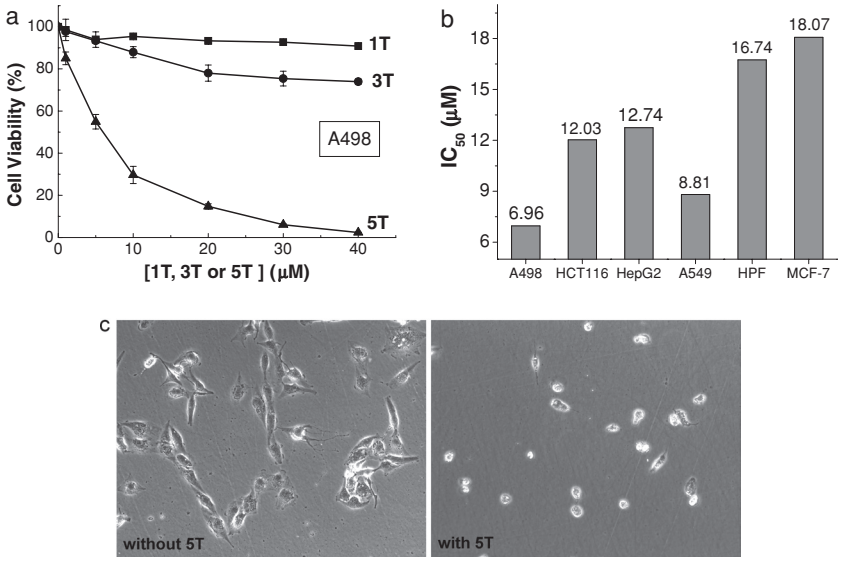

Figure 1. a) Cell viability of A498 treated with **1T**, **3T**, and **5T** using a typical MTT assay. Error bars correspond to standard deviations from three separate measurements. b) IC_{50} values of **5T** to different cell lines. c) Phase contrast images of A498 treated with and without 5T (20 μM) for 48 h.

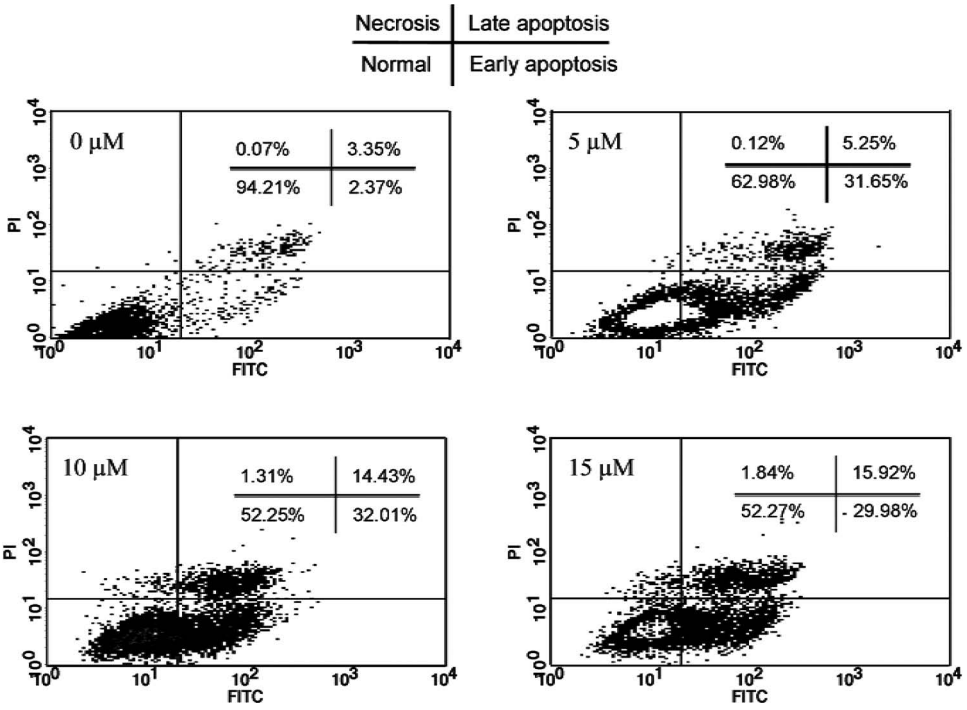

Figure 2. Apoptosis and necrosis of A498 cells analyzed by flow cytometry. Cells were treated with **5T** (0–15 μM) for 24 h and double stained with Annexin V-FITC and PI dye. Reported values are the means ± SD ($n = 3$).

on the structure of **5T** is needed to increase selective cytotoxicity to cancer cells over normal cells. The phase contrast images of A498 cells were taken before and after incubation with **5T** for 48 h. As shown in Figure 1c, upon incubating with **5T** (20 μM) for 48 h, the density of A498 cells is obviously less than that without **5T** and the cellular morphology or reduced cell size indicates that the cells are dead or in the late stage of apoptosis.[13] This result is consistent with MTT experiment.

To further study the anticancer mechanism of **5T**, we performed apoptosis assay of A498 cells after incubation with **5T** for 24 h by flow cytometry. Cells were double stained with fluorescein-labeled Annexin V (Annexin V-FITC) and PI dye. **Figure 2** shows the effect of **5T** on percentage of normal, early apoptotic, late apoptotic, and necrotic cells. The proportion of apoptotic cells is increased in a dose-dependent manner. Especially, at 10 μM of **5T**, the percentages of apoptotic and dead cells are 47.8%. Thus, the cytotoxicity of **5T** results in efficient cell apoptosis.

To confirm the apoptosis mechanism of **5T**, its target imaging of organelle was firstly investigated by confocal laser scanning microscopy (CLSM). In these experiments, two-color colocalizations of **5T** with organelle-specific dye were investigated. As shown in **Figure 3**a, the representative image of **5T** is green, the organelle-specific dye is red and the overlapped image is yellow. The fluorescence image of A498 cells stained with mitochondrial dye (mitotracker) completely overlapped with that stained with **5T**, which means that **5T** can selectively target mitochondria when it diffuses into the cell. To further confirm the apoptosis pathways of **5T**, apoptosis associated proteins in A498 cells were triggered before and after incubation with **5T**. As shown in Figure 3b, significant changes were detected in the expression of caspase-3, caspase-9, Bcl-2, Bax, JNK, and XIAP of the cells after treatment with **5T**. Both caspase-3 and -9 are mitochondria-mediated caspases and caspases-3 can be activated by initiator caspase-9.[14] The c-jun N-terminal kinase (JNK) represents a group of mitogen-activated protein kinases (MAPKs) involved in many cellular responses including apoptosis.[15] Bcl-2 and Bax are belonging to the antiapoptotic sub-group and the pro-apoptotic sub-group of the Bcl-2 protein family, respectively.[14] The members of Bcl-2 family are required for JNK-dependent apoptosis where JNK can indirectly inhibit Bcl-2 or directly inactivate its anti-apoptosis function through phosphorylation of Bcl-2.[16–18] XIAP is a member inhibitor of apoptosis protein, which would exert antiapoptotic effects by preventing the caspase activation.[14] Our results indicate that the apoptosis of cells by **5T** is associated with JNK pathway. As shown in Figure 3c, once JNK is activated, it can activate the pro-apoptotic protein Bax, whereby Bax translocation from cytosol to mitochondria associating with the subsequent activation of caspase-9 followed by downstream activation of caspase-3 to induce cell apoptosis.

The uptake mechanism of **5T** into cells was investigated. To probe whether **5T** was taken up by a passive diffusion or active transport mechanism, the A498 cells were co-incubated with **5T** and general endocytosis inhibitor, cytochalasin B that can block the formation of contractile microfilaments and inhibits the endocytosis process.[6,19] As shown in **Figure 4**, the cytochalasin B does not show any inhibition of **5T** uptake, which means the **5T** enters the cell mainly by a passive diffusion mechanism.

Anticancer nanodrugs are rapidly progressing due to the enhanced permeability and retention effect that increases antitumor efficacy. Combinations of anticancer drugs are commonly used in medicine to broaden antitumor spectrum and generate synergistic effects.[20] Up to now, most nanodrugs

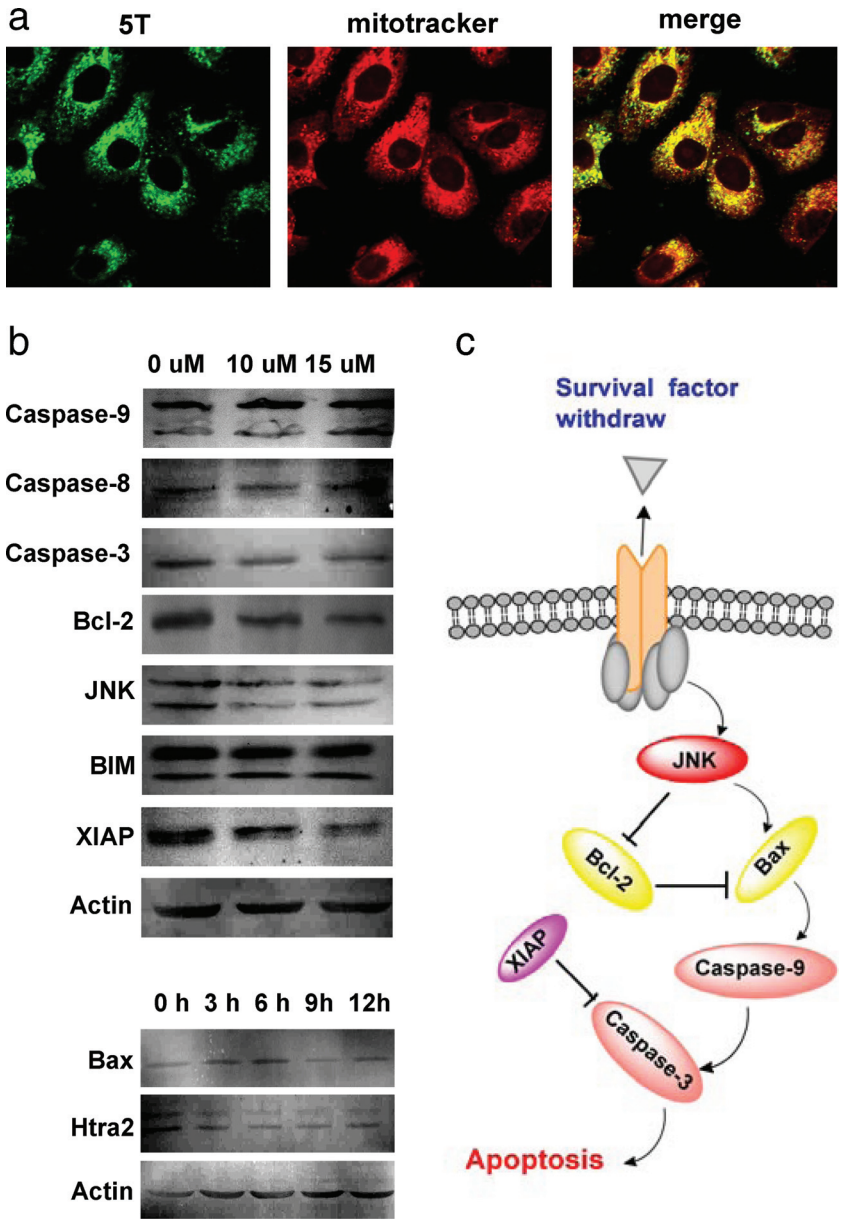

Figure 3. a) Fluorescence images of A498 cells stained with mitochondrial dye, **5T**, and the overlapped image. The representative image of **5T** is green, the organelle-specific dye is red and the overlapped image is yellow. b) Expression regulations of apoptosis associated proteins in A498 cells induced by **5T**. A498 cells were incubated with or without **5T** at varying concentrations (0–15 μM) or incubation times (0–12 h). c) The proposed mitochondria-mediated apoptosis pathway of A498 cancer cells induced by **5T**.

are designed by loading anticancer drugs to nanoparticles that act as delivery system.[21] Recent studies show that nanoparticles with a negative or positive surface charge can be prepared through electrostatic interactions.[22,23] Thus, the preparation of nanodrugs by electrostatic interactions of cationic anticancer drug with anionic one provides a previously untapped expanse of anticancer drug combinations, and offers an opportunity to generate unexpected synergistic effects. The preparation of nanodrug by electrostatic interactions of cationic **5T** with anionic one was performed and the synergistic effects of the anticancer drug combination were examined. The DNA-alkylation agent, chlorambucil,[11] was used as negatively charged compensation pair to **5T**. As reported, the delivery of chlorambucil specifically to mitochondria increases activity by 100 fold through retargeting from the nucleus to the mitochondria.[11] Thus, the enhanced anticancer activity of **5T**-chlorambucil combination is expected. **Scheme 2**a shows the chemical structures of **5T**-chlorambucil complexes, where the **5T** with different molar amounts of sodium chlorambucil in water gives 1:1 to 1:5 complexes under vigorously stirring through the electrostatic interactions. Scanning electron microscopy (SEM) shows the formation of **5T**-chlorambucil nanoparticles. As shown in Scheme 2b, the 1:4 complex forms nanoparticles in water with the size of about 50 nm. The similar nanoparticles were also obtained for other complexes (Figure S2, Supporting Information). As noted that the chlorambucil itself forms large aggregates at the same concentration; while no obvious nanoparticles are observed for **5T** itself (Figure S2, Supporting Information). The target imaging of organelle by the complex (1:4) was also investigated by confocal laser scanning microscopy. As shown in Scheme 2c, the complexes retain the ability of mitochondria imaging. The anticancer activities of these nanoparticles together with **5T** and chlorambucil themselves were determined by MTT assay (Figure S3, Supporting Information) and the IC_{50} values were calculated and summarized in **Table 1**. The chlorambucil does not show obvious anticancer activity towards all cell lines; while all the five **5T**-chlorambucil nanoparticles show effective suppression of cell growth in all cell lines. The nanoparticles exhibit 2–9-fold more cytotoxicity than free **5T**. Especially, the complexes show remarkably strong cytotoxicity against MCF-7 cells that are the worst sensitive to **5T** among the cell lines and 9-fold more cytotoxicity is observed than free **5T**.

It is reported that free small molecular drug can be recognized by P-glycoprotein and pumped out of a cell as quickly as they cross through the outer membrane of cells, which leads to anticancer drug resistance. However, nanoparticle cannot be easily pumped out because they are encapsulated in the cellular compartments.[24] On the one hand, **5T** can directly target mitochondria after diffusing into the cell and efficiently kill cancer cells, and the nanoparticles can not be easily pumped out. On the other hand, mitochondria targeting of **5T**-chlorambucil nanoparticles can significantly increases the anticancer activity of chlorambucil. Thus, the enhanced anticancer activity of **5T**-chlorambucil nanoparticles is attributed to the synergistical anticancer activity of **5T** and chlorambucil. As the

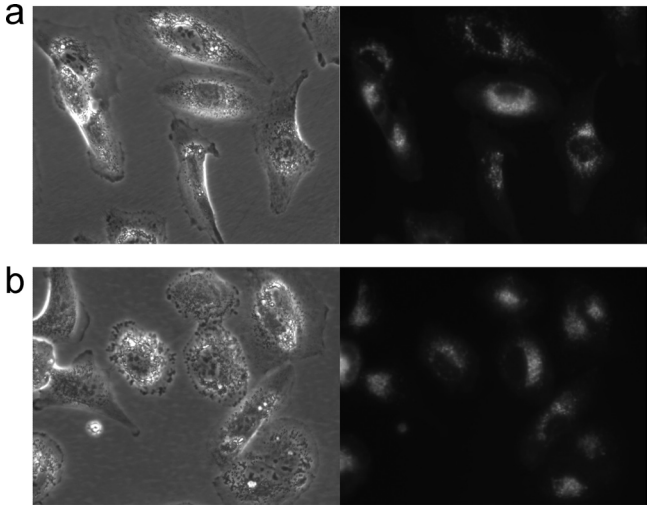

Figure 4. a) Phase contrast bright-field images of A498 cells (left) and their fluorescence images (right) in the presence of **5T**. b) Phase contrast bright-field images of A498 cells (left) and their fluorescence images (right) in the presence of **5T** and cytochalasin B. The cells were precultured in DMEM medium with cytochalasin B (1 μg mL^{-1}) at 37 °C for 2 h and then 20 μM **5T** was added. After 12 h, the cells were washed once with 1 × PBS buffer and images were taken with 300 ms exposure time. The false color of **5T** is green and the type of light filter is D380/15 nm exciter, 420 nm beamsplitter, and D460/25 nm emitter.

highly hydrophobic, densely packed structure of the inner mitochondrial membrane is impenetrable to most small molecular drugs, the difficulty of accessing the mitochondrial has limited the targeting of therapeutics.[11] The success of **5T**-chlorambucil nanoparticles provides an initial attempt to design and synthesis of new anticancer drug that targets mitochondria.

Table 1. IC_{50} values of **5T** -chlorambucil nanoparticles (μM).

	A498	A549	MCF-7	HPF	HCT116
5T:chlorambucil (1:1)	2.60	5.86	2.68	7.05	5.66
5T:chlorambucil (1:2)	2.54	5.28	2.29	7.01	5.95
5T:chlorambucil (1:3)	2.61	4.94	2.27	7.02	5.11
5T:chlorambucil (1:4)	2.11	3.37	1.97	6.90	4.91
5T:chlorambucil (1:5)	2.45	4.57	2.43	7.79	6.04
5T	6.96	8.81	18.07	16.74	12.03
chlorambucil	50	50	50	50	50

3. Conclusions

In conclusion, cationic oligothiophenes **5T** was firstly discovered with both anticancer activities and molecular imaging properties. **5T** can selectively accumulate in mitochondria and efficiently induce apoptosis of cells associating with JNK pathway activation. Compared with other oligomeric thiophene compounds with anticancer activity, **5T** is a promising multifunctional efficient anticancer agent that incorporates optical monitoring capabilities and anticancer activity by targeting mitochondria. Besides, complexes through electrostatic interactions between **5T** and sodium chlorambucil (a widely used anticancer drug) with varying molar ratios were prepared. The complexes form nanoparticles in water with the size of about 50 nm. The **5T**-chlorambucil nanoparticles enhance anticancer activity by 2–9-folds due to the synergistical anticancer activity of **5T** and chlorambucil. Noted that **5T** shows similar cytotoxic activity against cancerous and normal cell lines. To solve this problem, linking the target group to **5T** to selectively bind to cancer cells or further optimization on the structure of **5T** is needed to increase selective cytotoxicity to cancer cells over normal cells. These findings may open a new door for the design and synthesis of new multifunctional anticancer drugs and the future development of nanotherapeutics.

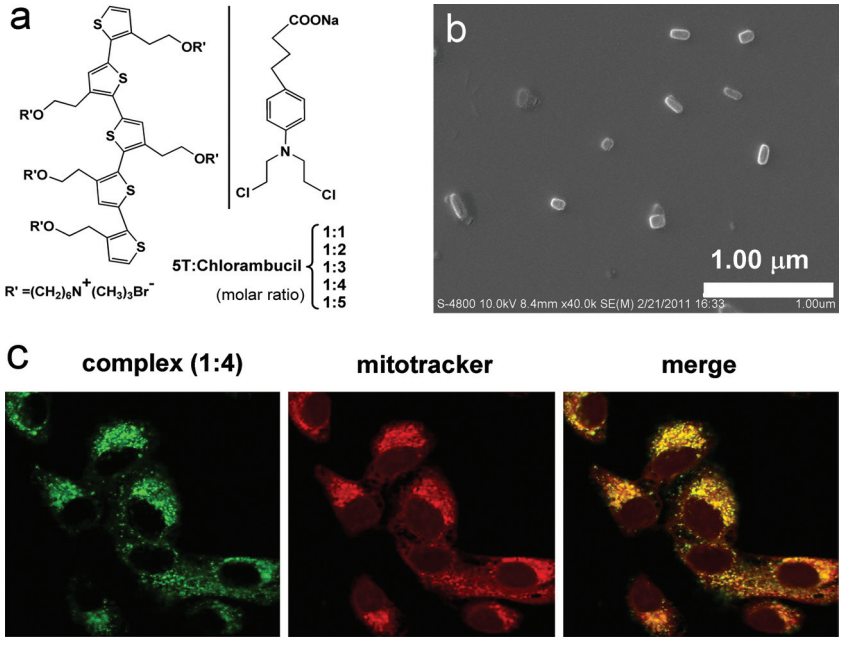

Scheme 2. a) The **5T** -chlorambucil complexes with varying molar ratio from 1:1 to 1:5. b) Scanning electron microscopy image of **5T** -chlorambucil complex (1:4). c) Fluorescence images of A498 cells stained with mitochondrial dye, complex (1:4), and the overlapped image. The representative image of complex (1:4) is green, the organelle-specific dye is red and the overlapped image is yellow.

4. Experimental Section

Materials: All the reagents and solvents used were commercially available. Fetal bovine serum (FBS) was purchased from Sijiqing Biological Engineering Materials (Hangzhou, China). MTT was obtained from Xinjingke Biotech (Beijing, China) and dissolved in 1×PBS before use. Human embryo lung diploid cell (HPF), pulmonary adenocarcinoma cell (A549), renal cell carcinoma (A498), hepatoblastoma G2 cell (HepG2), human breast cancer cell (MCF-7) and colon carcinoma (HCT116) were purchased from cell culture center

of Institute of Basic Medical Sciences, Chinese Academy of Medical Sciences (Beijing, China) and cultured in Dulbecco's Modified Eagle's Medium (DMEM) supplemented with 10% FBS, 4500 mg L^{-1} glucose and 4.0 mM glutamine. The water was purified using a Millipore filtration system. The cell apoptosis detection kit (including Annexin V-FITC, PI and binding buffer) was obtained from KeyGen Biotech Company Limited (Nanjing, China). The cell mitochondria dye Mito Tracker Red CMXRos (M7512) was purchased from Invitrogen. 3,3′,5,5′-tetramethylbenzidine (TMB) was purchased from Sigma.

Measurements: The ^{1}H NMR and ^{13}C NMR spectra were recorded on a Bruker Avance 400 MHz spectrometer. Elemental analysis was carried out with a Flash EA1112 instrument. The fluorescence spectra were measured on a Hitachi F-4500 fluorometer with a xenon lamp as excitation source. UV–vis absorption spectra were taken on a Jasco V-550 spectrometer. Phase contrast bright-field images were taken with fluorescence microscope (Olympus I × 71) with a mercury lamp (100 W) as light source. SEM images were taken on Hitachi S-4800 scanning electron microscopy. The absorbance for MTT analysis was recorded on a microplate reader (BIO-TEK Synergy HT) at a wavelength of 520 nm. Confocal laser scanning microscopy (CLSM) characterization was conducted by a confocal laser scanning biological microscope (FV1000-IX81, Olympus). Flow cytometric analysis was taken by flow cytometry (FACSCalibur, BD).

Synthesis of 3-(2-(6-Bromohexyloxy)ethyl)thiophene, ***2***: The 2-(thiophen-3-yl)ethanol **1** (663 µL, 6 mmol) was added to a suspension of sodium hydride (70% in oil dispersion, 206 mg, 6 mmol) in dry DMF under nitrogen. After the solution had been stirred for 30 min, 1,6-dibromohexane (4.6 mL, 10 mmol) was added to the solution by syringe at room temperature. After stirring overnight, the reaction was quenched by adding water. The mixture was extracted with CH_2Cl_2 for three times. The combined organic layer was washed with brine, dried over $MgSO_4$, concentrated under vacuum, and purified by silica chromatography with petroleum ether/ethyl acetate (40:1) as eluent to give an oil (0.54 g, 31%). ^{1}H NMR (400MHz, $CDCl_3$, δ) 1.61–1.45 (m, 4H), 1.72(p, 2H, J = 6.78), 1.99 (p, 2H, J = 6.82), 3.04 (t, 2H, J = 6.98), 3.53 (t, 2H, 6.86), 3.57 (t, 2H, J = 6.50), 3.76 (t, 2H, J = 7.01), 7.15–7.10 (m, 2H), 7.37 (m, 1H). ^{13}C NMR (75MHz, $CDCl_3$, δ) 25.43, 28.01, 29.57, 30.83, 32.79, 33.82, 70.77, 71.03, 121.04, 125.14, 128.53, 139.46. HR-MS (EI): Calcd. for $C_{12}H_{19}BrOS$: 290.0340, 292.0320; Found: 290.0342, 290.0316.

Synthesis of 2-Bromo-3-(2-(6-bromohexyloxy)ethyl)thiophene, ***3***: To a solution of **2** (2.65 g, 9.1mmol) in 108 ml DMF, N-bromosuccinimide (NBS) (1.62 g, 9.1 mmol) in 54 mL DMF was added. The mixture was stirred at room temperature for 24 h in dark, after which the mixture was poured into 100 mL of distilled water and extracted with *n*-pentane three times. The combined organic layer was washed with water (3 × 15 mL) and $NaHCO_3$(aq) (2 × 50 mL), dried over anhydrous $MgSO_4$, concentrated under vacuum, and purified by silica chromatography with petroleum ether/ethyl acetate (40:1) as eluent to give an oil (2.80 g, 83%). ^{1}H NMR (400 MHz, $CDCl_3$, δ) 7.18 (d, J = 5.3, 1H), 6.86 (d, J = 5.3, 1H), 3.58 (t, J = 6.8, 2H), 3.49 –3.35 (m, 4H), 2.84 (t, J = 6.7, 2H), 1.84 (dd, J = 13.5, 6.6, 2H), 1.65–1.50 (m, 2H), 1.50–1.29 (m, 4H). ^{13}C NMR (100 MHz, $CDCl_3$, δ) 138.57, 128.73, 125.35, 109.91, 70.77, 69.78, 33.97, 32.82, 30.09, 29.58, 28.03, 25.43. EI-MS (m/z): 370.0.

Synthesis of 2-Pinacolboryl-3-(2-(6-bromohexyloxy)ethyl)thiophene, ***4***: 1.04 mL (2.83 mmol) of *n*-butyllithium (2.72 M in hexane) was added to a solution of **3** (1.00 g, 2.7 mmol) in 20 mL THF at –78 °C by syringe. The mixture was stirred at –78 °C for 2 h, then 2-isopropoxy-4,4,5,5,-tetramethyl-1,3,2-dioxaborolane (0.7 mL, 3.38 mmol) was added to the solution. The mixture was stirred at –78 °C for another 1 h, warmed to room temperature. After stirring for further 12 h, the mixture was poured into water, extracted with ether, dried over anhydrous $MgSO_4$, concentrated under vacuum, and purified by silica chromatography with petroleum ether/ethyl acetate (40:1) as eluent to give an oil (0.57 g, 51%). ^{1}H NMR (400 MHz, $CDCl_3$, δ) 7.50 (d, J = 3.8, 1H), 7.07 (d, J = 3.8, 1H), 3.61 (t, J = 6.9, 2H), 3.43 (dt, J = 13.5, 6.2, 4H), 3.18 (t, J = 6.8, 2H), 1.93–1.80 (m, 2H), 1.64–1.53 (m, 2H), 1.51–1.36 (m, 4H), 1.33 (s, 12H). ^{13}C NMR (100 MHz, $CDCl_3$, δ) 150.34, 131.49, 130.82, 83.71, 71.81, 70.54, 33.95, 32.82, 30.75, 29.63, 28.05, 25.46, 24.86. EI-MS (m/z): 416. Anal. Calcd. for $C_{18}H_{30}BBrO_3S$: C 51.82, H 7.25; Found C 51.85, H 7.13.

Synthesis of 2,5-Dibromo-3-(2-(6-bromohexyloxy)ethyl)thiophene, ***5***: Compound **2** (1.00 g, 3.43 mmol) was dissolved in THF and acetic acid (12 mL, 1:1, v/v). NBS (1.22 g, 6.85 mmol) was added to the solution in one portion, and the mixture was stirred for 1 h, after which the mixture was poured into 30 mL of distilled water and extracted with n-pentane three times. The combined organic layer was washed with water (3 × 15 mL) and $NaHCO_3$(aq) (2 × 50 mL), dried over anhydrous $MgSO_4$, concentrated under vacuum, and purified by silica chromatography with petroleum ether/ethyl acetate (40:1) as eluent to give an oil (1.38g, 90%). ^{1}H NMR (400 MHz, $CDCl_3$, δ) 6.87 (s, 1H), 3.56 (t, J = 6.5, 2H), 3.42 (dd, J = 11.6, 5.7, 4H), 2.79 (t, J = 6.5, 2H), 1.95–1.79 (m, 2H), 1.65-1.51 (m, 2H), 1.51–1.30 (m, 4H).^{13}C NMR (100 MHz, $CDCl_3$, δ) 139.75, 131.53, 110.43, 109.03, 70.83, 69.49, 34.03, 32.82, 30.13, 29.55, 28.03, 25.46. EI-MS (m/z): 448. Anal. Calcd. for $C_{12}H_{17}Br_3OS$: C, 32.10; H, 3.82. Found: C, 32.05; H 4.01.

*Synthesis of 7-(2-(Thiophen-3-yl)ethoxy)heptanyltrimethylammonium bromide (****1T****)*: To a solution of **2** (291 mg, 1 mmol) in 0.5 mL THF was added 3 mL of trimethylamine aqueous solution. The mixture was allowed to stir at 40 °C for 24h. The excess trimethylamine was removed under reduced pressure. The resulting solid dissolved in CH_3OH was triturated with Et_2O to give a white solid (0.31 g, 89%). ^{1}H NMR (400MHz, $CDCl_3$, δ) 7.27(m, 1H), 7.02–6.98 (m, 2H), 3.65–3.56 (m, 4H), 3.47 (m, 11H), 2.91 (t, 2H, 6.78), 1.75 (br, 2H), 1.58 (br, 2H), 1.42 (br, 4H). ^{13}C NMR (75MHz, $CDCl_3$, δ) 23.02, 25.76, 25.81, 29.25, 30.61, 53.27, 66.64, 70.37, 70.79, 120.96, 125.10, 128.48, 139.34. ESI-MS (m/z): 270.2. Anal. Calcd. for $C_{15}H_{28}BrNOS$: C, 51.42; H, 8.06; N, 4.00. Found: C, 51.11; H, 7.95; N, 4.12.

Synthesis of Compound ***6***: To a solution of **5** (230 mg, 0.51 mmol), potassium carbonate (566 mg, 4.09 mmol) and tetrakis(triphenylphosphine) palladium(0) (100 mg, 0.09 mmol) in toluene/water (4 mL, v/v 3:1) was added 2-bithienyl boronate ester **4** (485 mg, 1.17 mmol) in THF (3 mL) in one portion. The mixture was degassed by bubbling nitrogen for 20 min and stirred under reflux for further 20 h. After cooling down to room temperature, 15 mL of water was added. The mixture was extracted with CH_2Cl_2, dried over anhydrous $MgSO_4$, concentrated under vacuum, and purified by silica chromatography with petroleum ether/ethyl acetate (500:35) as eluent to afford a solid (303 mg, 68%). ^{1}H NMR (400 MHz, $CDCl_3$, δ) 7.31 (s, 1H), 7.18 (s, 1H), 7.07 (s, 1H), 7.03 (s, 1H), 6.99 (d, J = 2.9, 1H), 3.65 (s, 2H), 3.55 (s, 4H), 3.44 (s, 2H), 3.39 (s, 10H), 3.06 (s, 2H), 2.83 (s, 2H), 2.77 (s, 2H), 1.84 (s, 6H), 1.55 (s, 6H), 1.43 (s, 6H), 1.36 (s, 6H). ^{13}C NMR (100 MHz, $CDCl_3$, δ) 139.27, 139.04, 135.89, 135.71, 131.74, 130.34, 129.62, 129.15, 129.09, 128.02, 125.87, 123.90, 70.86, 70.80, 70.72, 33.94, 32.79, 29.59, 29.44, 28.04, 25.45. MS (MALDI-TOF): 870.3(M), 790.3(M-Br). Anal. Calcd. for $C_{36}H_{53}Br_3O_3S$: C, 49.72; H, 6.14. Found: C, 49.76; H, 6.23.

Synthesis of Oligomer ***3T***: The **3T** was prepared from **6** as the previous synthesis procedure for **1T** in 93% yield. ^{1}H NMR (400 MHz, MeOD, δ) 7.54 (d, J = 3.9, 1H), 7.40 (d, J = 3.8, 1H), 7.24 (s, 1H), 7.17 (d, J = 3.9, 1H), 7.12 (d, J = 3.9, 1H), 3.80–3.69 (m, 2H), 3.65 (s, 4H), 3.58–3.44 (m, 6H), 3.40 (s, 6H), 3.19 (s, 27H), 3.11 (s, 2H), 2.87 (s, 2H), 2.82 (s, 2H), 1.81 (s, 6H), 1.63 (s, 6H), 1.45 (s, 12H). ^{13}C NMR (100 MHz, CD_3OD, δ) 139.64, 139.20, 136.08, 135.73, 131.22, 130.29, 129.48,128.97, 128.63, 128.03, 125.93, 124.03, 70.41, 70.35, 70.30, 70.25, 66.45, 59.26, 52.28, 29.11, 25.76, 25.54, 25.48, 22.58. ESI-MS (m/z): 269.1(M-3Br), 443.7 (M-2Br).

Synthesis of Compound ***7***: To a solution of **6** (107 mg, 0.123 mmol) in 5 mL DMF was added dropwise NBS (44 mg, 0.247 mmol) in 10 mL DMF at –20 °C over 5 min. The mixture was stirred for 2 h, then warmed to room temperature and stirred over night. The resulted mixture was poured into water, extracted with ether, dried over anhydrous $MgSO_4$, concentrated under vacuum, and purified by silica chromatography with petroleum ether/ethyl acetate (500:35) as eluent to afford a solid (110 mg, 93%). ^{1}H NMR (400 MHz, $CDCl_3$, δ) 7.02 (s, 2H), 6.97 (s, 1H), 3.61 (d, J = 5.8, 2H), 3.53 (d, J = 6.7, 4H), 3.40 (s, 12H), 2.97 (s, 2H), 2.75 (s, 4H), 1.85 (d, J = 5.7, 6H), 1.56 (dd, J = 12.9, 6.5, 6H), 1.50–1.29 (m, 12H).

^{13}C NMR (100 MHz, $CDCl_3$, δ) 140.18, 140.09, 136.68, 135.07, 133.03, 132.91, 131.94, 130.29, 128.73, 128.39, 112.45, 110.70, 70.89, 70.85, 70.83, 70.56, 70.46, 70.34, 33.90, 32.75, 29.70, 29.55, 29.51, 29.38, 29.33, 28.02, 27.98, 25.46, 25.43. MS (MALDI-TOF): 1026.2 (M), 948.3 (M-Br), 868.4 (M-2Br). Anal. Calcd. for $C_{36}H_{51}Br_5O_3S$: C, 42.08; H, 5.00. Found: C, 42.52; H, 5.18.

Synthesis of Compound ***8***: Compound **8** was prepared from **4** (100 mg, 0.239 mmol) and **7** (107 mg, 0.104 mmol) as above synthesis procedure for **6.** Purification by silica chromatography with petroleum ether/ethyl acetate (500:40) as eluent to give a solid (103 mg, 68%). ^{1}H NMR (400 MHz, $CDCl_3$, δ) 7.19 (d, J = 4.3, 2H), 7.10 (d, J = 3.9, 2H), 7.05 (s, 1H), 7.00 (d, J = 4.4, 2H), 3.67 (t, J = 7.0, 6H), 3.59 (t, J = 6.4, 4H), 3.52–3.29 (m, 20H), 3.07 (s, 6H), 2.83 (t, J = 6.2, 4H), 1.84 (dd, J = 12.9, 6.3, 10H), 1.58 (d, J = 6.2, 10H), 1.40 (dd, J = 10.5, 6.2, 20H). ^{13}C NMR (100 MHz, $CDCl_3$, δ) 139.64, 136.28, 136.25, 136.03, 135.95, 135.81, 134.18, 131.76, 131.67, 130.48, 129.51, 129.40, 129.15, 128.21, 128.09, 124.16, 71.07, 71.00, 70.86, 70.83, 70.68, 34.06, 32.91, 30.08, 29.95, 29.75, 29.71, 28.18, 28.14, 25.62, 25.56, MS (MALDI-TOF): 1448.4 (M), 1366.4 (M-Br). Anal. Calcd. for $C_{60}H_{87}Br_5O_3S$: C, 49.76; H, 6.06. Found: C, 49.67; H, 6.06.

Synthesis of Oligomer ***5T***: **5T** was prepared from **8** as above synthesis procedure for **1T** in 90% yield. ^{1}H NMR (400 MHz, MeOD, δ) 7.46 (s, 2H), 7.34 (s, 1H), 7.31 (s, 1H), 7.27 (s, 1H), 7.16 (d, J = 2.5, 2H), 3.79 (s, 6H), 3.71 (s, 4H), 3.62–3.49 (m, 10H), 3.42 (s, 10H), 3.20–3.23 (m, 45H), 3.14 (s, 6H), 2.91 (s, 4H), 1.83 (s, 10H), 1.68 (s, 10H), 1.48 (d, J = 5.2, 20H).^{13}C NMR (100 MHz, MeOD, δ) 140.12, 136.92, 136.39, 136.31, 136.16, 135.43, 134.09, 131.08, 130.97, 130.49, 130.46, 129.35, 129.01, 128.58, 128.16, 128.11, 124.27, 70.48, 70.40, 70.31, 70.26, 70.13, 66.42, 58.84, 52.35, 29.60, 29.52, 29.48, 29.22, 29.18, 25.79, 25.60, 25.50, 22.66, 22.63. ESI-MS (m/z): 268.9 (M-5Br), 356.3 (M-4Br), 501.2 (M-3Br).

Preparation of ***5T****-Chlorambucil Complexes*: To a solution of **5T** (2.41 mg, 1.38 μmol) in 5 mL of water was dropwise added sodium chlorambucil (0.450 mg, 1.38 μmol) in 5 mL of water. The mixture was vigorously stirred for 48 h, and concentrated under lyophilization to less than 2 mL. The resulted 1:1 complex of **5T**-chlorambucil was fixed 2 mL and directly used in following experiments. The 1:2 to 1:5 complexes of **5T**-chlorambucil were prepared as the same procedure for 1:1 complex only by varying the concentration of sodium chlorambucil (0.9 mg, 2.76 μmol; 1.35 mg, 4.14 μmol; 1.35 mg, 5.52 μmol; 2.25 mg, 6.90 μmol) in water.

Assay for Cell Viability by MTT: Six kinds of cells were routinely grown in DMEM medium containing 10% FBS and then harvested for subculture using trypsin (0.05%, Gibco/Invitrogen) and grown in a humidified atmosphere containing 5% CO2 at 37 °C. Cells were subcultured in 96-well plates the day before the experiment at a density of $4 \sim 7 \times 10^4$ cells mL^{-1}. Upon culture for further 24 h, **1T**, **3T**, **5T** or **5T**-chlorambucil complexes with varying concentrations were respectively added into the cells followed by further culture for 48 h, then the culture media were discarded and MTT (1 mg mL^{-1}, 100 μL per well) was added to the wells followed by incubation at 37 °C for 4 h. The supernatant was abandoned, then 150 μL DMSO per well was added to dissolve the produced formazan and the plates were shaken for an additional 10 min. The absorbance values of the wells were then read with microplate reader at a wavelength of 520 nm. The cell viability rate (VR) was calculated according to the following equation, where the control group was carried out in the absence of the drugs. IC_{50} values were analyzed by the statistic software SPSS (Version 13.0).

$$VR(\%) = \frac{A_{\text{experimental group}}}{A_{\text{control group}}} \times 100\%$$

In Vitro Imaging of the Apoptosis of A498 Cells by ***5T***: The A498 cells were seeded in 35 mm culture plates (Nunc) at a density of approximately 8×10^4 cells per plate for 24 h, and then the cells were washed once with 1 × PBS and then grown in 1 mL DMEM medium with and without **5T** (20 μM). Phase contrast images were taken at 48 h using fluorescence microscopy (Olympus I×71).

Confocal Laser Scanning Microscopy (CLSM) Measurements: A498 cells were seeded onto 35 mm Petri dishes with glass bottoms and allowed to incubate for 24 h for attachment, after which cells were treated with complex (1:4) or **5T** (10 μM) for 12 h. The cell staining and fixation were processed according to manufacturer's protocol. In short, the cell mitochondria dye, mitotracker (M7512, Invitrogen, 100 nM) was used to stain the cells for 15 min. After fixation with 4% formaldehyde for 15 min, the cells were then examined by confocal laser scanning microscopy using a 405 nm laser for **5T** and 559 nm laser for mitochondria dye. The fluorescence of **5T** was highlighted in green and mitochondria dye in red.

Western Blot Analysis: Samples containing 30 μg of total protein were resolved by a 12% SDS-PAGE gel, and then transferred onto PVDF membranes (Amersham Pharmacia Biotech). The membranes were blocked with 5% non-fat dry milk in purified water for 2 h, and incubated with the desired primary antibody overnight: caspase-3, caspase-9, caspase-8, Htra2, Bim, Bcl-2, Bax, JNK, β-actin, XIAP. Subsequently, the membrane was incubated with appropriate horseradish peroxidase-conjugated secondary antibodies (Tiangen Biotech Co. China) for 2 h. The color reaction was developed with tetramethylbenzidine (TMB, Sigma).

Apoptosis Analysis by Flow Cytometry: Apoptosis was determined by staining cells with Annexin V-FITC and PI, because Annexin V can identify the externalization of phosphatidylserine during the apoptotic progression and therefore detect early apoptotic cells. The cell apoptosis detection kit was used to quantitate the apoptosis of cells. Flow cytometry (FCM) was used to calculate the percentage of apoptotic cells. The pre-prepared cell suspensions were directly analyzed using 488 nm laser. Cell fragments were excluded with forward and side-scatter gating to ensure that all detected signals originated from relatively intact cells; signals from FITC and PI were individually recorded in Channel FL-1 and FL-2. The flow cytometry diagrams presented were obtained from a population of 3×10^4 cells.

Supporting Information

Supporting Information is available from the Wiley Online Library or from the author.

Acknowledgements

The authors are grateful to the National Natural Science Foundation of China (Nos. 21033010, 21003140, 90913014, 21021091) and the Major Research Plan of China (No. 2012CB932600, 2011CB808400).

Received: July 30, 2011
Revised: September 15, 2011
Published online: December 13, 2011

[1] J. Kim, Y. Piao, T. Hyeon, *Chem. Soc. Rev.* **2009**, *38*, 372.
[2] J. Kim, *Adv. Mater.* **2008**, *20*, 478.
[3] H. Kobayashi, P. L. Choyke, *Acc. Chem. Res.* **2011**, *44*, 83.
[4] V. Bagalkot, L. Zhang, E. Levy-Nissenbaum, S. Jon, P. W. Kantoff, R. Langer, O. C. Farokhzad, *Nano Lett.* **2007**, *7*, 3065.
[5] J. K. Willmann, N. van Bruggen, L. M. Dinkelborg, S. S. Gambhir, *Nat. Rev. Drug. Discov.* **2008**, *7*, 591.
[6] L. Liu, M. Yu, X. Duan, S. Wang, *J. Mater. Chem.* **2010**, *20*, 6942.
[7] N. R. Krishnaswamy, T. R. Seshadri, B. R. Sharma, *Tetrahedron Lett.* **1966**, 4227.
[8] J. B. Hudson, *Antivir. Res.* **1989**, *12*, 55.
[9] W.-C. Xu, C. L. Ashendel, C.-t. Chang, C.-j. Chang, *Bioorg. Med. Chem. Lett.* **1999**, *9*, 2279.

[10] A. Gazit, P. Yaish, C. Gilon, A. Levitzki, *J. Med. Chem.* **1989**, *32*, 2344.
[11] S. B. Fonseca, M. P. Pereira, R. Mourtada, M. Gronda, K. L. Horton, R. Hurren, M. D. Minden, A. D. Schimmer, S. O. Kelley, *Chem. Biol.* **2011**, *18*, 445.
[12] F. Denizot, R. Lang, *J. Immunol. Methods* **1986**, *89*, 271.
[13] D. W. Nicholson, *Nature* **2000**, *407*, 810.
[14] G. Kroemer, L. Galluzzi, C. Brnnner, *Physiol. Rev.* **2007**, *87*, 99.
[15] R. J. Davis, *Cell* **2000**, *103*, 239.
[16] M. Faris, N. Kokot, K. Latinis, S. Kasibhatla, D. R. Green, G. A. Koretzky, A. Nel, *J. Immunol.* **1998**, *160*, 134.
[17] K. Lei, A. Nimnual, W. X. Zong, N. J. Kennedy, R. A. Flavell, C. B. Thompson, *Mol. Cell. Biol.* **2002**, *22*, 4929.
[18] K. Yamamoto, H. Ichijo, S. J. Korsmeyer, *Mol. Cell. Biol.* **1999**, *19*, 8469.
[19] Z. Darzynkiewicz, *Cytometry.* **1997**, *27*, 1.
[20] R. A. Petros, J. M. DeSimone, *Nat. Rev. Drug Discovery* **2010**, *9*, 615.
[21] K. Cho, X. Wang, S. Nie, Z. Chen, D. Shin, *Clin. Cancer Res.* **2008**, *14*, 1310.
[22] X. Feng, Y. Tang, X. Duan, L. Liu, S. Wang, *J. Mater. Chem.* **2010**, *20*, 1312.
[23] S. Cafaggi, E. Russo, R. Stefani, R. Leardi, G. Caviglioli, B. Parodi, G. Bignardi, D. D. Totero, C. Aiello, M. Viale, *J. Controlled Release* **2007**, *121*, 110.
[24] Y. J. Son, J. S. Jang, Y. W. Cho, H. Chung, R. W. Park, I. C. Kwon, I. Kim, J. Y. Park, S. B. Seo, C. R. Park, S. Y. Jeong, *J. Controlled Release* **2003**, *91*, 135–145.